Int. J. Electrochem. Sci., 13 **(2018)** 7590 – 7597, doi: 10.201964/2018.08.25

International Journal of
ELECTROCHEMICAL
SCIENCE
www.electrochemsci.org

Electrochemical Performances and Air Stability of Fe-doped CoS_2 Cathode Materials for Thermal Batteries

Tianlang Yu[1], *Zhiyong Yu*[1,*], *Yong Cao*[2,*], *Hanxing Liu*[1], *Xiaojiang Liu*[2],*Yixiu Cui*[2], *Chao Wang*[2], *Yanhua Cui*[2]

[1] School of Materials Science and Engineering, Wuhan University of Technology, Wuhan, 430070, China
[2] Institute of Electronic Engineering, China Academy of Engineering Physics, Mianyang, 621900, China
[*]E-mail: yuzhiyong@whut.edu.cn, yongcao2011d@126.com

Received: 16 April 2018 / *Accepted:* 26 May 2018 / *Published:* 5 July 2018

In this work, Fe-doped CoS_2 ($Co_xFe_{1-x}S_2$) compounds were synthesized and evaluated as cathode materials for thermal batteries. The results verified bimetallic disulfides exhibited more balanced properties on the air stability and thermal stability compared to monometallic disulfides. Interestingly, a remarkable improvement in discharge performances could be achieved in bimetallic disulfide. The cells with bimetallic disulfides showed lower resistances and weakened polarization peak in comparison to that of CoS_2, which could contribute to the decrease in particle size and the variation in intermediate phase compositions during discharge, thus leading to better discharge performances. Moreover, S-$Co_{0.3}Fe_{0.7}S_2$ displayed significantly better discharge performances than other investigated stored-disulfides, which implied bimetallic disulfide could achieve superior electrochemical performances even being stored under air at high relative humidity. Therefore, the strategy of using bimetallic disulfides offers an attractive way to explore promising cathode materials for thermal batteries.

Keywords: Thermal batteries, $Co_xFe_{1-x}S_2$, Air stability, Electrochemical performance, Hydrothermal

1. INTRODUCTION

The demands for power sources with high reliability, long storage life, high power density and energy density in oil/gas borehole, space exploration and military application have promoted the development of thermal batteries, which are activated by heating the solid salt electrolyte to liquid state (usually at 450-550^oC) [1-6]. FeS_2 is currently widely used as cathode material due to its low

cost, high discharge capacity, steady voltage and good compatibility with molten salt [7-10]. In spite of the success of FeS_2, the exploration of new cathode materials is still an enormous challenge to fulfil the strong requirement of thermal batteries with high power and long-life.

Current researches have been focused on the CoS_2 material[11-14], which exhibits a longer discharge life and more extraordinary ability of pulse current load due to its higher thermal decomposition temperature (650^{o}C vs 550^{o}C, decompose in N_2) and higher conductivity compared with FeS_2 [15-17]. However, the CoS_2 suffers from the drawback of poor stability under ambient atmosphere, which may result in capacity degradation of batteries due to the formation of $CoSO_4 \cdot H_2O$.

Bimetallic disulfides have been widely studied in the fields of super capacitors and electro-catalysis because they may display more balanced or improved performances compared to the corresponding monometallic compounds [18-20]. This study explored the possibility of using bimetallic disulfide as cathode materials for thermal batteries. The evaluation of electrochemical performances and air stability of Fe-doped CoS_2 cathode materials was presented. For comparisons, the individual disulfides CoS_2 and FeS_2 were also analyzed.

2. EXPERIEMTAL

2.1 Materials preparation and characterization

For preparation of the $Co_xFe_{1-x}S_2$ ($0 \leqslant x \leqslant 1$), $CoCl_2 \cdot 6H_2O$, $FeCl_2 \cdot 4H_2O$, S, $Na_2S \cdot 9H_2O$ were used as the raw materials. The $Co_xFe_{1-x}S_2$ precursors were synthesized by a hydrothermal method as described in previous work [10] by controlling molar ratio of Co/Fe = 1:0, 0.7:0.3, 0.3:0.7, 0:1 and pH=5. The obtained precursors were heated at 510°C for 5h under argon to produce the samples of $Co_xFe_{1-x}S_2$. To investigate the air stability of $Co_xFe_{1-x}S_2$, the as prepared samples were stored in air (25°C, 100% relative humidity) for 7 days. The corresponding stored samples were labeled as S-$Co_xFe_{1-x}S_2$.

The crystal structure was characterized by X-ray diffraction (XRD, X'Pert PRO) using Cu-Kα radiation. The morphology and particle size were investigated using scanning electron microscope (SEM, Ultra 55). The thermal stability was examined by thermogravimetry (TG, NETZSCH STA 449F3) with a heating rate of 10°C/min in argon.

2.2 Electrochemical measurements

For assembling a cell, the current collector (graphite paper), anode (Li-Si alloy), separator (50wt.% of MgO and 50wt.% of LiCl-KCl) and cathode (80 wt.% of $Fe_xCo_{1-x}S_2$ and 20wt.% of separator) were layered in a die and then pressed to a pellet(Φ22mm). The cells were tested by an electrochemical test instrument (CT2001B, Land) at 525℃ in a drying room.

The cell resistance (R_{cell}) is calculated based on the following equation with the change of current and voltage in a pulse discharge test [14-15].

$$R_{cell} = \delta V_{pulse}/\delta I_{pulse} \quad (1)$$

3. RESULTS AND DISCUSSION

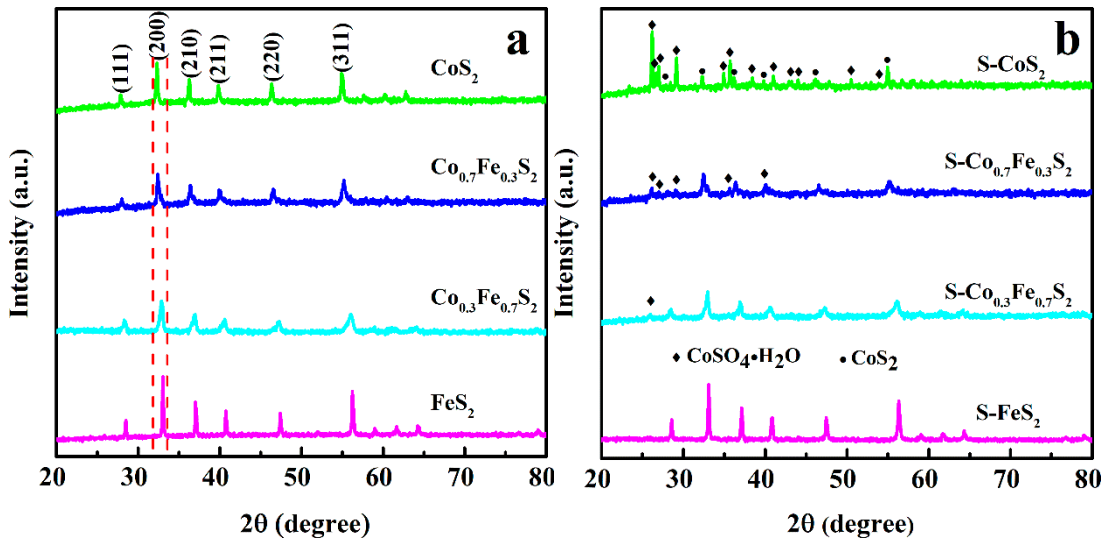

Figure 1. XRD patterns of $Co_xFe_{1-x}S_2$ (a) and S-$Co_xFe_{1-x}S_2$ (b)

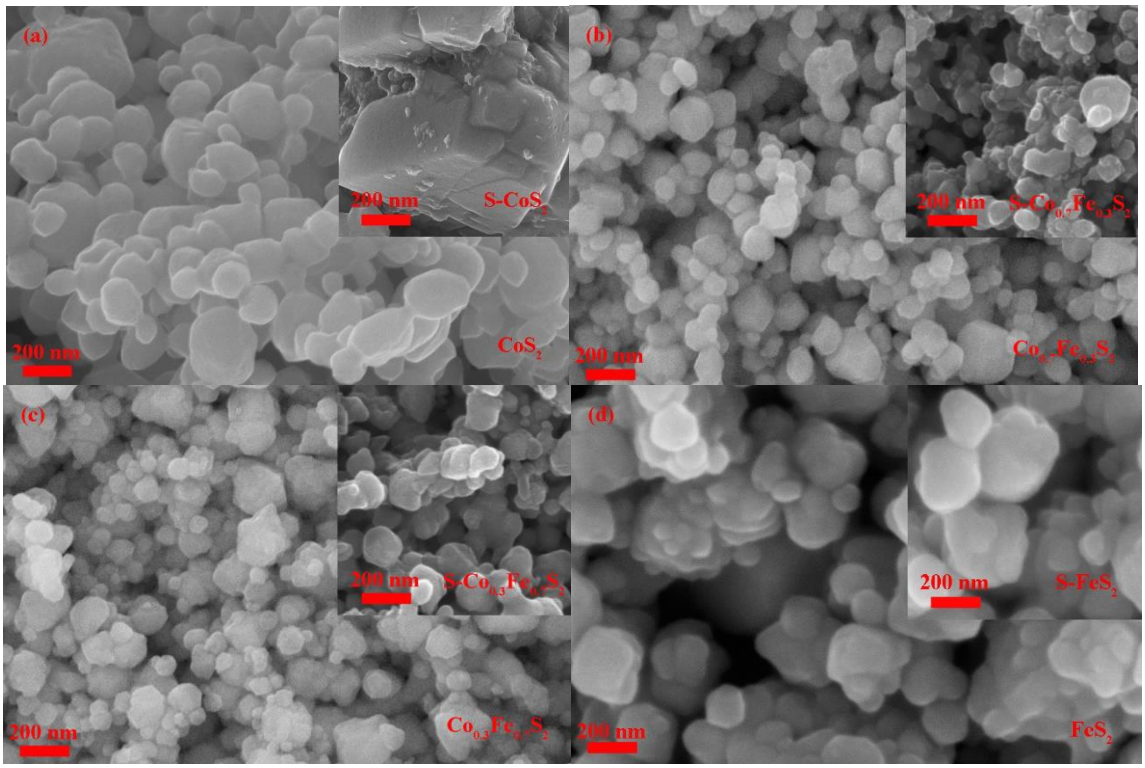

Figure 2. SEM images of CoS_2(a), $Co_{0.7}Fe_{0.3}S_2$(b), $Co_{0.3}Fe_{0.7}S_2$(c), FeS_2(d). Insets: the corresponding stored samples

The XRD patterns of $Co_xFe_{1-x}S_2$ and their stored samples are shown in Fig. 1. As seen in Fig. 1a, the diffraction peaks of CoS_2 are corresponding to cubic cobalt disulfide (CoS_2, PDF#19-0362). With the addition of Fe element, the peaks of samples gradually shift to high angle and finally index to pyrite FeS_2 (FeS_2, PDF#71-0053). After being stored, no apparent impurities or secondary phase are observed in the S-FeS_2 sample, while one weak peak related to $CoSO_4$•H_2O appears in the pattern of S-$Co_{0.3}Fe_{0.7}S_2$. With further increase of Co content, especially for the S-CoS_2, obvious diffraction peaks of $CoSO_4$•H_2O are presented. These results reveal better air stability of bimetallic disulfides than that of CoS_2.

The SEM images of $Co_xFe_{1-x}S_2$ are shown in Fig. 2. For comparisons, the insets of Fig. 2a-d give the SEM images of the corresponding stored-samples. Bimetallic disulfides present smaller particle size (see Fig. 1b and Fig. 1c) than that of monometallic disulfides (see Fig. 2a and Fig. 2d). Obviously, the storage causes a change in morphology and an increase in size for the CoS_2 particles (inset of Fig. 1a). The rougher surface and more apparent aggregation of particles can be observed after being stored for $Fe_{0.3}Co_{0.7}S_2$ (see Fig. b). Moreover, no noticeable change on morphology and particle size occurs for the rest of stored-samples. The above SEM results imply that $Co_xFe_{1-x}S_2$ series perform obviously different air stability.

TG curves of the bimetallic disulfides, FeS_2 and CoS_2 are compared in Fig. 3. CoS_2 shows a typical three stages decomposition behavior, relating to the formation of sulfates for its poor air stability. For Fe-contained samples, the similar feature of TG curves with only one stage decomposition suggests the better air stability of bimetallic disulfides than that of CoS_2, which agrees well with the results of XRD and SEM. The decomposition temperature of FeS_2, $Co_{0.3}Fe_{0.7}S_2$ and $Co_{0.7}Fe_{0.3}S_2$ were about 570 °C, 600°C and 620 °C, respectively, revealing a better thermal stability of the bimetallic disulfides in comparison to FeS_2.

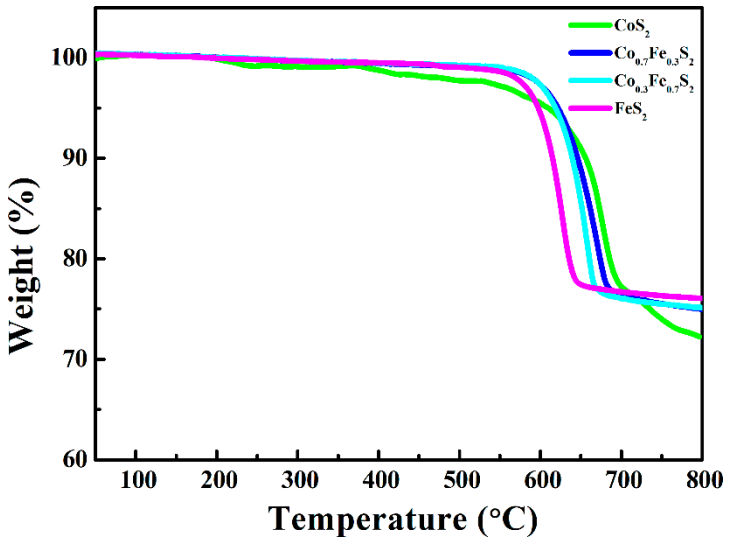

Figure 3. TG curves of $Co_xFe_{1-x}S_2$ with a heating rate of 10°C/min in argon

Fig. 4 shows the discharge profiles for various samples at a current density of 100 mA/cm^2. As shown, the CoS_2, $Co_{0.7}Fe_{0.3}S_2$, $Co_{0.3}Fe_{0.7}S_2$ and FeS_2 can deliver discharge capacities of 695 mAh/g, 710 mAh/g, 730 mAh/g and 685 mAh/g, respectively, indicating that Co/Fe ratio has an important effect on the discharge capacities of the samples. Notably, the $Co_{0.3}Fe_{0.7}S_2$ can achieve significantly improved discharge capacities compared to the monometallic compounds, which is even higher than that of CoS_2/CNT (669mAh/g) reported by S. Xie et al. [12].

According to the discharge mechanisms, the phase conversion processes for CoS_2 and FeS_2 proceed as following: $CoS_2 \rightarrow Co_3S_4 \rightarrow Co_9S_8 \rightarrow Co$ [14], and $FeS_2 \rightarrow Li_3Fe_2S_4 \rightarrow Li_2FeS_2 \rightarrow Fe$ [2, 21]. Although the discharge mechanism for FeS_2 differs from that for CoS_2, they both show a three-step conversion reaction. As shown in Fig.4, the CoS_2 and FeS_2 obtained in our work also show three-step discharge behaviors. It can be found that the FeS_2 shows higher voltage at the first step but drop to lower voltage at the second step in comparison to CoS_2. At the last discharge step, the two samples show almost same voltage. Furthermore, the discharge profile of the $Co_{0.7}Fe_{0.3}S_2$ combines the features of CoS_2 and FeS_2, which exhibits a four-step discharge behavior including two long and two short discharge plateaus. However, the $Co_{0.3}Fe_{0.7}S_2$ seemingly shows a three-step discharge behavior. The discharge plateau of $Co_{0.3}Fe_{0.7}S_2$ related to the conversion reaction from Co_3S_4 to Co_9S_8 disappears, which may be caused by the ignorable discharge capacity due to low content of Co at this step.

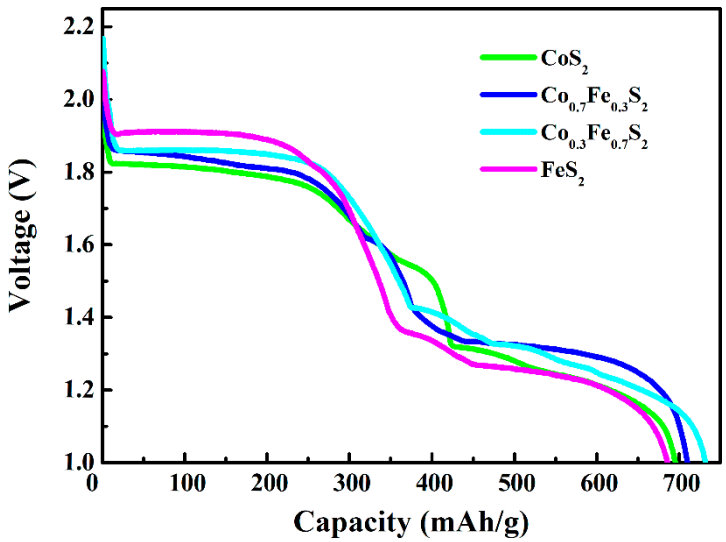

Figure 4. Discharge profiles of $Co_xFe_{1-x}S_2$ at a current density of 100 mA/cm^2

The discharge performance of $Co_xFe_{1-x}S_2$ is also investigated by a pulse mode with 1s pulse of 500 mA/cm^2 after each 30s background current density of 100 mA/cm^2 (see Fig. 5). The CoS_2, $Co_{0.7}Fe_{0.3}S_2$, $Co_{0.3}Fe_{0.7}S_2$ and FeS_2 can output 20, 21, 24 and 17 pulses, respectively. In comparison to FeS_2, the CoS_2 shows better pulse performance, which is corresponding to previous work [16]. Moreover, the bimetallic disulfide $Co_{0.3}Fe_{0.7}S_2$ displays a significant advantage in pulse performance compared to CoS_2.

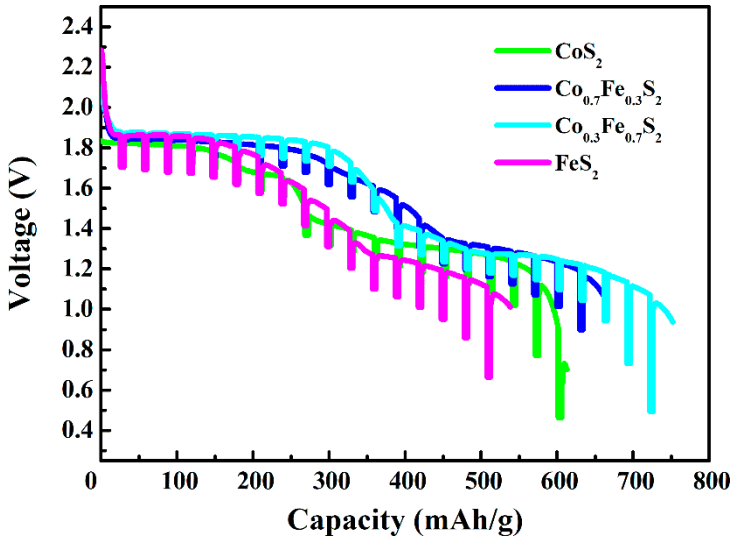

Figure 5. Discharge performance of $Co_xFe_{1-x}S_2$ with 1s pulse of 500 mA/cm^2 after each 30s background current density of 100 mA/cm^2

The cell resistance plays a key factor in the discharge capability of disulfides. The calculated cell resistances based on the data of Fig.5 are summarized in Fig. 6. As seen, the resistance of FeS_2 cell is much higher than that of other compounds during discharge. It implies a high electronic resistance of FeS_2, which causes a poor discharge performance compared to CoS_2 and bimetallic disulfides. Besides, the resistance curves of bimetal disulfides and CoS_2 cells are almost overlapped at the beginning of discharge. With discharge proceeding, the resistances of bimetallic disulfide cells are lower than that of CoS_2. Notably, an obvious peak appears in resistance curve of CoS_2 cell, which contributes to the formation of Co_3S_4 phase with high electronic resistance.

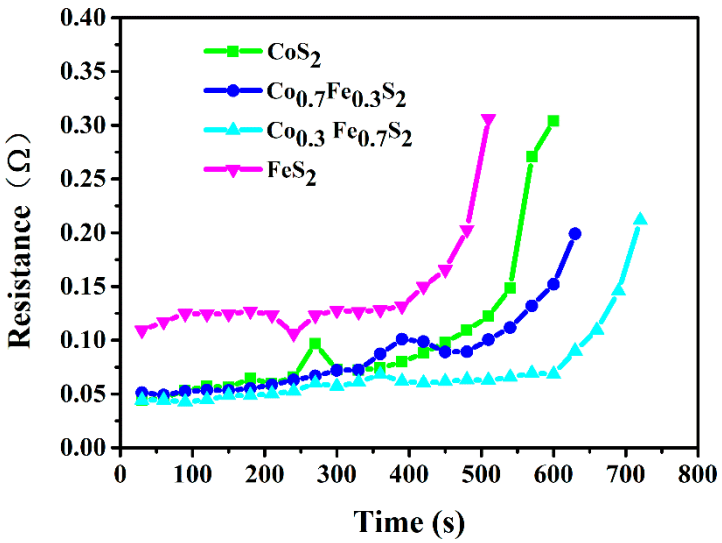

Figure 6. Resistances of $Co_xFe_{1-x}S_2$ cells

Similarly, C.Y. Jin et al. also found that the conductivity of intermediate phase affected the electrochemical behavior of disulfide [1]. Furthermore, it can be found that the bimetallic disulfides,

especially for $Co_{0.3}Fe_{0.7}S_2$, show weakened resistance peaks, which may be caused by the decrease of particle size and different intermediate phase compositions during discharge [1, 10], thus leading to better discharge performances. Firstly, better contact between molten electrolytes and cathode materials due to smaller particle size will decrease the polarization of cells. Secondly, the lower polarization of cells with bimetallic disulfides also can be attributed to the lower proportion of the intermediate phase Co_3S_4 during discharge.

Discharge performances of S-$Co_xFe_{1-x}S_2$ are presented in Fig.7. As shown in Fig. 7a, the discharge capacities of CoS_2 and S-$Co_{0.7}Fe_{0.3}S_2$ distinctly decrease to 145 mAh/g and 475 mAh/g due to the formation of a large amount of $CoSO_4$•H_2O, while the S-$Co_{0.3}Fe_{0.7}S_2$ and S-FeS_2 can still deliver specific discharge capacities of 640 mAh/g and 620 mAh/g. Although the FeS_2 shows the best discharge capacity retention after being stored, the S-$Co_{0.3}Fe_{0.7}S_2$ display the highest discharge capacity. Regarding the pulse discharge performance, the FeS_2 only decreases 1 pulse, while striking reduction of 14 pulses has been found for the CoS_2 after being stored. The S-$Co_{0.7}Fe_{0.3}S_2$ and S-$Co_{0.3}Fe_{0.7}S_2$ can still output 15 and 21 pulses, which is closed to or evidently higher than that of S-FeS_2. These results indicate that the air stability makes a significant impact on the discharge performances of the disulfides. Bimetallic disulfides with suitable Fe content can achieve superior air stability and discharge performances, which would be favorable for the application in thermal batteries.

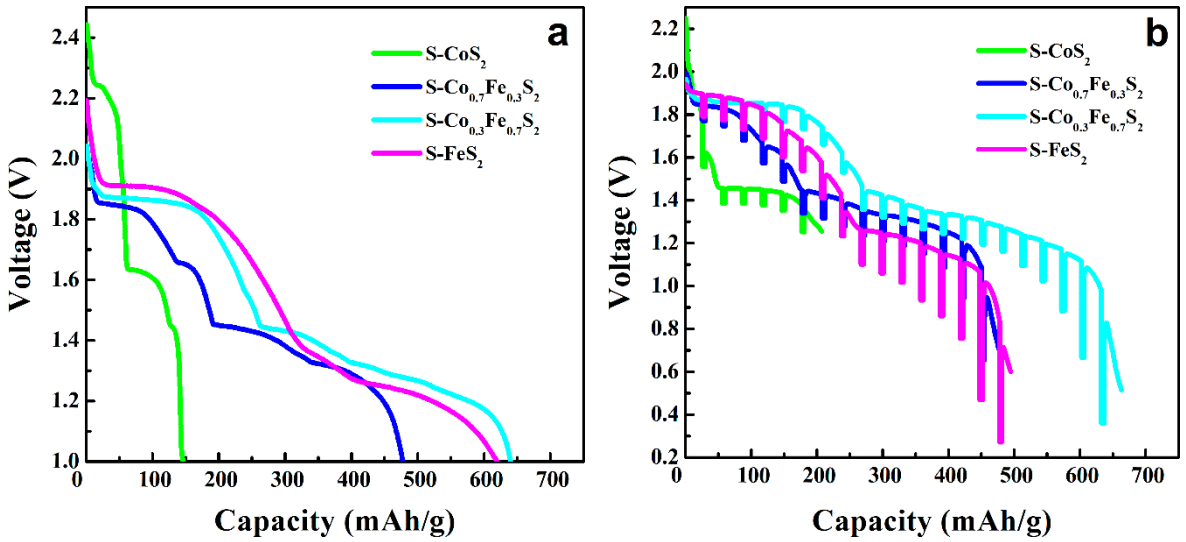

Figure 7. Discharge performances of S-$Co_xFe_{1-x}S_2$ at a current density of 100 mA/cm^2 (a), with 1s pulse of 500 mA/cm^2 after each 30s background current density of 100 mA/cm^2 (b)

4. CONCLUSIONS

Cathode materials $Co_xFe_{1-x}S_2$ were successfully synthesized via a hydrothermal method. The thermal stability of the $Co_xFe_{1-x}S_2$ compounds decreased with increasing Fe content. However, Fe doping greatly improved the air stability and the discharge performances of CoS_2. The $Co_{0.3}Fe_{0.7}S_2$

showed the best discharge performance among investigated samples. This improvement in discharge performance could contribute to the lower polarization and weakened polarization peak during discharge, which may relate to the reduction of particle size and different intermediate phase compositions. Even being stored in air at 100% relative humidity for 7 days, the S-$Co_{0.3}Fe_{0.7}S_2$ still exhibited better discharge performance compared to S-FeS_2. Therefore, the development of bimetallic disulfides provides a potential approach to overcome the shortcomings of monometallic disulfides for application in thermal batteries.

ACKNOWLEDGEMENTS
This work was supported by Natural Science Foundation of China (No.21703215).

References

1. C.Y. Jin, L.P. Zhou, L.C. Fu, J.J. Zhu, D.Y. Li, W.L. Yang, *J. Power Sources*, 352 (2017) 83.
2. P. Zhang, J.S. Liu, Z.T. Yang, X.J. Liu, F. Wang, *Electrochim. Acta*, 230 (2017) 358.
3. Y.Q. Niu, Z. Wu, J.L. Du, W.Y. Duan, *J. Power Sources*, 245 (2014) 537.
4. Y.S. Choi, H.R. Yu, H.W. Cheong, *J. Power Sources*, 276 (2015)102.
5. R.A. Guidotti, P. Masset, *J. Power Sources*, 161 (2006) 1443.
6. P. Masset, R.A. Guidotti, *J. Power Sources*, 164 (2007) 397.
7. J. Ko, I.Y. Kim, H. Cheong, Y.S. Yoon, *J. Am. Ceram. Soc.*, 100 (2017) 4435.
8. S.H. Kang, J. Lee, T.U. Hur, H.W. Cheong, J. Yi, *Int. J. Electrochem. Sci.*, 11 (2016) 4371.
9. Y.S. Choi, S.B. Cho, Y.S. Lee, *J. Ind. Eng. Chem.*, 20 (2014) 3584.
10. Z.T. Yang, X.J. Liu, X.L. Feng, Y.X. Cui, X.Y. Yang, *J. Appl. Electrochem*. 44 (2014) 1075.
11. Y.L. Xie, Z.J. Liu, H.L. Ning, H.F. Huang, L.B. Chen, *RSC Adv.*, 8 (2018) 7173.
12. S. Xie, Y.F. Deng, J. Mei, Z.T. Yang, W.M. Lau, H. Liu, *Compos. Part B*, 93 (2016) 203.
13. H.Y. Huang, J.L. Gao, L.P. Zhang, H.R. Hu, K. Zhu, *ECS Trans.***,** 32 (2011) 295.
14. P.J. Masset, R.A. Guidotti, *J. Power Sources*, 178 (2008) 456.
15. P.J. Masset, R.A. Guidotti, *J. Power Sources*, 177 (2008) 595.
16. P. Butler, C. Wagner, R. Guidotti, I. Francis, *J. Power Sources*, 136 (2004) 240.
17. R.A. Guidotti, F.W. Reinhardt, J. Dai, D.E. Reisner, *J. Power Sources*, 160 (2006) 1456.
18. S.Y. Huang, D. Sodano, T. Leonard, S. Luiso, P.S. Fedkiw, *J. Electrochem. Soc.*, 4 (2017) F276.
19. G.L. Li, C.L. Xu, *Carbon* 90 (2015) 44.
20. L. Jin, B. Liu, Y. Wu, S. Thanneeru, J. He, *ACS Appl. Mater. Interfaces*, 42 (2017) 36837.
21. B. Czajka, M. Zieliński, M. Wojciechowska, I.T. Foralewska, *J. Solid State Electrochem.*, 18 (2014) 2351.